Closest Spectral Fit for Removing Clouds and Cloud Shadows

Qingmin Meng, Bruce E. Borders, Chris J. Cieszewski, and Marguerite Madden

Abstract

Completely cloud-free remotely sensed images are preferred, but they are not always available. Although the average cloud coverage for the entire planet is about 40 percent, the removal of clouds and cloud shadows is rarely studied. To address this problem, a closest spectral fit method is developed to replace cloud and cloud-shadow pixels with their most similar non-clouded pixel values. The objective of this paper is to illustrate the methodology of the closest spectral fit and test its performance for removing clouds and cloud shadows in images. The closest spectral fit procedures are summarized into six steps, in which two main conceptions, location-based one-to-one correspondence and spectral-based closest fit, are defined. The location-based one-to-one correspondence is applied to identify pixels with the same locations in both base image and auxiliary images. The spectral-based closest fit is applied to determine the most similar pixels in an image. Finally, this closest spectral fit approach is applied to remove cloud and cloud-shadow pixels and diagnostically checked using Landsat TM images. Additional examples using QuickBird and MODIS images also indicate the efficiency of the closest spectral fit for removing cloud pixels.

Introduction

A significant obstacle to extracting information from remotely sensed images is the presence of clouds and their shadows. The average cloud coverage for our entire planet is about 40 percent (Simonett, 1983). Sometimes cloudy images have to be used because they are all that are available. For example, satellite multispectral scanner images of the Earth's surface such as Landsat images are often corrupted by clouds because of nadir-only observing satellites having relatively infrequent revisiting periods (Song and Civco, 2002).

Mitchell *et al.* (1977) developed a cloud distortion model and filtering procedures to remove cloud cover in satellite images. Liu and Hunt (1984) and Chanda and Majumder (1991) further improved the distortion model and filtering procedures. However, their methods are used for removing thin clouds, and it is difficult to determine the range of cloud densities in which clouds and cloud shadows (CCS) are removed efficiently.

Qingmin Meng is with the Center for Applied GIScience, University of North Carolina at Charlotte, Charlotte, NC 28223 (qmengl@uncc.edu).

Bruce E. Borders, and Chris J. Cieszewski are with the Warnell School of Forestry and Natural Resources, University of Georgia, Athens, GA 30602 (qmeng@uga.edu).

Marguerite Madden is with the Department of Geography, University of Georgia, Athens, GA 30602.

Cihlar and Howarth (1994) and Simpson and Stitt (1998) developed special methods for detecting and removing cloud contamination from AVHRR images. These methods are not suitable for removing CCS in other satellite imagery. For example, one prerequisite of their methods is that there is at least one single maximum or a single minimum for the seasonal trajectory of a satellite-derived variable (Mitchell *et al.*, 1977).

The multi-date effect brightness correction method (Caselles, 1989) is another approach to removing CCS. Song and Civco (2002) used this method to replace CCS with appropriate pixel values. In essence, this approach has an important assumption that the sample mean and standard deviation (SD) of band values in CCS imagery is as the same as the cloud-free imagery. It is apparent that the mean and SD can only be estimated as approximations for that image since CCS cover parts of the image; the bigger CCS areas in the imagery, the larger the difference between the estimated mean and SD and their real values.

This paper develops a closest spectral fit (CSF) technique for replacing CCS pixels with the most similar pixels at cloud-free areas in the same image. The CSF technique is applied to remove CCS pixels in Landsat-5 Thematic Mapper (Landsat TM) data, and then error diagnostics is conducted using the images of Landsat TM, QuickBird, and Moderate Resolution Imaging Spectroradiometer (MODIS) as examples.

Closest Spectral Fit Appr oach

Two satellite images covering the same area and acquired at different times are needed. The base image is the one with relatively less CCS, and should retain the information that is acquired. Also, the base image is the one to be used for further applications. The other image will be called the auxiliary image. As much as possible, cloudy areas in the base image should be cloud-free in the auxiliary image. There should be no overlap of cloud pixels or cloud-shadow pixels in the two images and both images are selected for this criteria based on a visual estimation. If there are overlaps of CCS pixels, we need select an additional auxiliary image, which can be used to remove the overlapped CCS pixels. Using only the base image, it is impossible to select the most similar pixels for the pixels whose signatures are distorted by cloud and cloud shadow, since CCS have corrupted the real energy received and recorded by the satellite sensor. The auxiliary image is used as a medium to determine the relationship in the base image of

Photogrammetric Engineering & Remote Sensing
Vol. 75, No. 5, May 2009, pp. 569–576.

0099-1112/09/7505–0569/$3.00/0
© 2009 American Society for Photogrammetry and Remote Sensing

the most similar pixels to those pixels whose signatures are distorted by clouds and cloud shadows.

A general process of applying the CSF method to remove CCS in images is developed, and this general process is depicted in Figure 1. The conceptions, algorithms and steps used for CSF are described as follows.

Step 1: Georegistration and Coregistration

The base and auxiliary satellite images often need to be geo-rectified. Often, U.S. Geological Survey (USGS) Digital Orthophoto Quarter-quads (DOQQs) are used as the source of control (i.e., root mean square errors should be less than 10 m). Then, coregistration is conducted to obtain good alignment.

Step 2: Surface reflectance Calibration

Raw satellite images with the spectral values represented with digital numbers (DN) often contain substantial noise.
To remove the noise, a surface reflectance calibration process may be implemented. For example, one way is to use the commercial package FLAASH to derive the surface reflectance from the raw images consistently (ITT Company, 2006).

It is not necessary to calculate the surface reflectance in this research. For example, Landsat TM images (Path/Row: 18/38) used as one example were bought from the USGS Earth Resource Observation System Data Center. The data had been corrected for the radiometric and geometric distortions of the images to the precision correction level before delivery.

Step 3: Knowledge-based CCS Detection

The visible and near-infrared bands are sensitive to clouds and cloud-shadows and can be used to detect CCS. For example, the bands 1, 3, and 4 of Landsat TM imagery are the best indicators for the detection of clouds and cloud shadows, respectively. Clouds are present when the digital numbers (DN) of band 1 exceeds a threshold (i.e., 95 for the Landsat-5 used here). Shadows are present when the value of band 4 is less than a threshold (i.e., 55 is used), and the ratio of band 4 to band 3 (i.e., 1.3 is used in this research) also is applied to help distinguish cloud shadows from water. Cloud shadows and water areas might have similar reflectance values in band 4. However shadow areas generally have much higher values in band 4 than those in band 3, while water areas have relatively close values in band 4 and band 3.

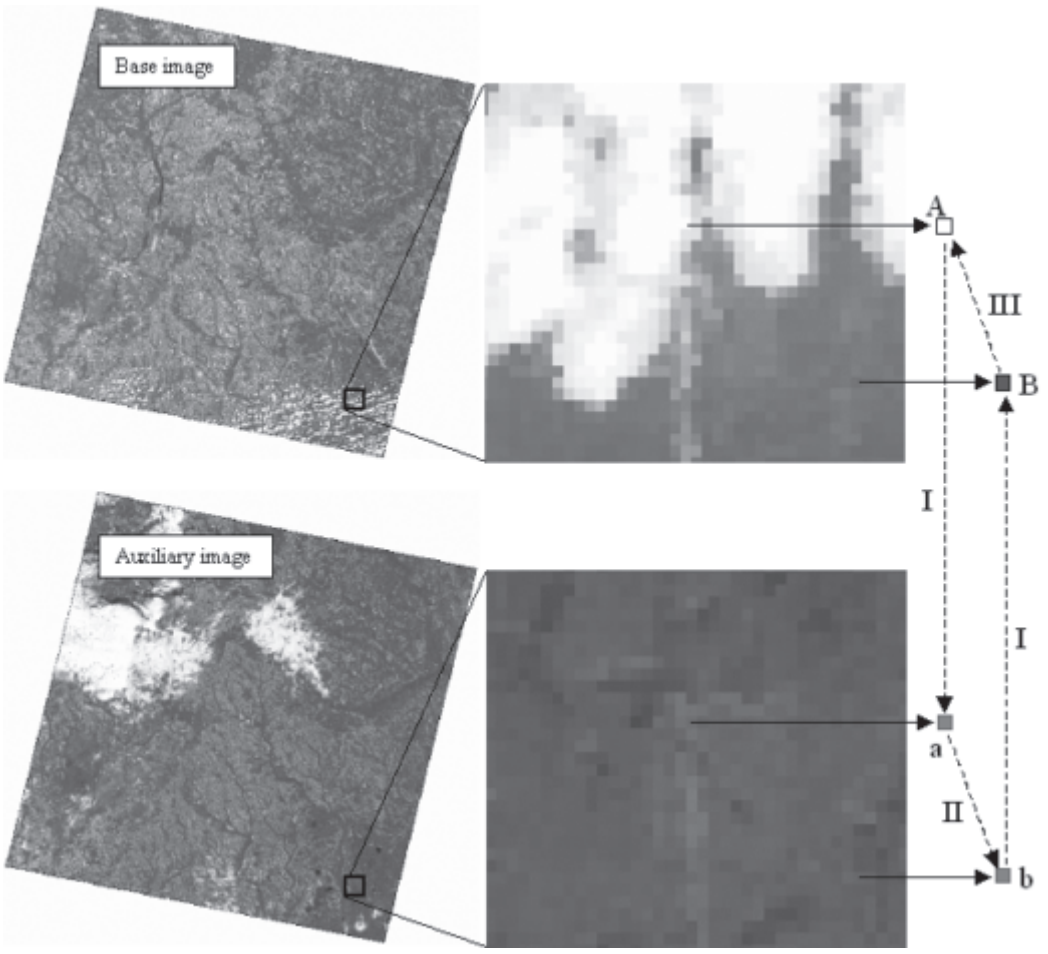

Figure 1. A diagram of cloud and cloud-shadow removal using closest spectral fit: I, location-based one-to-one correspondence, pixels $A \leftrightarrow a$, and pixels $B \leftrightarrow b$; II, closest spectral fit, pixels $a \leftrightarrow b$; III, the replacement of pixel A using its most similar pixel B according to the closest spectral fit of $A \leftrightarrow B$ based on the same relationship of $a \leftrightarrow b$. A color version of this figure is available at the ASPRS website: **www.asprs.org** .

The threshold of the ratio of band 4 to band 3 therefore is used to detect cloud shadows. The values of these thresholds might vary for images acquired at different times. The algorithms can be summarized as follows.

A. Algorithm for Identifying Cloud Pixels

If DN of TM band 1 > 95
Then cloud pixel
Set up a dataset for cloud pixel
Otherwise cloud-free pixel
Set up a dataset for cloud-free pixels

B. Algorithm for Identifying Cloud Shadow Pixel

If DN of TM band 4 < 55
    and ratio of (band4/band3) > 1.3
Then cloud shadow pixel
Set up a dataset for cloud shadow pixels

Step 4: Closest Spectral Fit

Closest spectral fit examines the distance between each pixel and the closest pixel to it in spectral space. In an image, if pixel *j* has the closest surface reflectance value to that of pixel *i*, then, *j* is called the closest spectral fit to pixel *i* (i.e., pixels *i* and *j* are more similar to each other than to any other pixels in this image). Similarly, based on the surface reflectance, the most similar pixel *b* in the auxiliary image can be identified for a given pixel *a*, in the auxiliary image (Figure1). In other words, in the auxiliary image the closest spectral fit analysis determines the most similar pixels (e.g., pixel *b*) to each of the pixels (e.g., pixel *a*) identified using location-based one-to-one correspondence to the CCS pixels (e.g., pixel *A*) in the base image in Step 3. The relationship of the most similar pixels *a* and *b* in the auxiliary image can be called closest spectral fit.

The distance from pixel to pixel measured in reflectance is a type of point-to-point distance. The smaller the distances are between pixels, the more similar the pixels are. Two pixels are identical to each other if the distance between them is 0. Euclidian distance (ED) is used in this CSF technique, since ED is widely applied in image processing and classification.

$$ED = \sqrt{\sum_{L=1}^{n} (i_L - j_L)^2} \quad (1)$$

where *ED* is the Euclidian Distance between pixels *i* and *j*, *L* indicates satellite bands, and *n* is the number of bands for the imagery being used, such as $n = 7$ for Landsat imagery. A SQL algorithm for the closest spectral fit can be summarized below.

SQL Algorithms for Closest Spectral Fit Analysis

```
sql;
sqrt ((a.band1-b.band1)* (a.band1-b.band1) + (a.band2-b.band2)*
    (a.band2-b.band2) + . . . + (a.bandm-b.bandm)* (a.bandm-b.bandm))
    as distance
from dataset.a, dataset.b
Set up dataset for closest spectral fit;
quit;
```

where dataset.a is the pixels in the auxiliary image having the same locations as CCS pixels in the base image, dataset.b is the cloud-free pixels in the auxiliary image, and *m* is band number of the image.

Step 5: Transfer of Closest Spectral Fit

When the relationship of closest spectral fit is built for pixels in the auxiliary image, we then transfer this to the base image using the location-based one-to-one correspondence between the base image and auxiliary image. For example in Figure 1, for pixels covered with CCS, we find pixel *A* (i.e., a given CCS pixel in the base image) and its location-based one-to-one correspondence pixel *a* (i.e., a pixel in the auxiliary image having the same location as *A*). We then find in the auxiliary image *a*'s most similar *b* (whose location-corresponding *B* in the base image must be cloud-free). By doing this we have built the relationship of closest spectral fit (i.e., the pixel *A* and *B*) in the base image. We then take advantage of the closest spectral fit in the base image by replacing the value of *A* in the base image with the value of *B*. The spectral integrity of the base image can be maintained because we use the most similar pixel B in the base image to replace the CCS pixel A in this image.

Step 6: Compose an Image in which Clouds and Cloud Shadows have been Removed

At last, an image in which CCS has been removed can be composed for the base image using remote sensing software. Filtering functions may need to be applied to obtain a smooth view of the composed image.

Case Studies

Example One: CCS Removal using Landsat TM Images

Two Landsat TM images, the base image (Path 18/Row 38, acquired on 07 August 2004) and the auxiliary image (Path 18/Row 38, acquired on 29 December 2004), were distributed by the U. S. Geological Survey (USGS) with precision correction (U.S. Geological Survey, 2006). Both images have areas covered with CCS, but we have determined visually that most of them are not overlapping. We need not conduct steps 1 and 2 discussed in the above section, because the images have been precisely corrected by USGS. Then, a SAS program was developed to conduct steps 3, 4, and 5, and then step 6 was implemented using ERDAS Imagine® 8.7 after the CCS pixels are replaced and the ASCII files are imported into ERDAS.

The results of replacing cloud and cloud-shadow pixels are pictured in Figure 2. Most of CCS are removed, but unsmooth views of the areas initially covered by CCS are achieved. A focal median analysis with a 3×3 size window using ERDAS Imagine® 8.7 was applied in order to smooth the images.

In the step of error diagnostics, we need to check the accuracy of the values of the replacement pixels. We randomly generated 10,000 pixels in the images (Figure 2). We deleted the 3,387 pixels that fell within the cloud and cloud shadow areas, and used the remaining 6,613 cloud-free pixels to check the accuracy of CCS removal. We first applied the CSF technique, i.e., we found pixel *A* (say, a given pixel in base image) and its location-corresponding *a* (say, a pixel in the auxiliary image having the same location as *A*). We found the most similar pixel *b* (say, a pixel in the auxiliary image) to *a* and found *b*'s location-corresponding *B* in the base image. Recalling that in the cloud removal procedure, *B* was used to replace the value of A (Figure 1), the objective now, this being the diagnostic check, is to examine the difference between the difference of DN between pixel *B* and pixel A.

We may wonder whether the CSF is as powerful as the simple approach of "cut and paste" using the non-clouded pixels in the auxiliary image to directly replace the CCS pixels in the base image. In other words, this cut and paste approach is to use pixel *a* to replace pixel *A* (Figure 1). The cut and paste approach is often used in practice, since it may be the easiest way. In order to check the efficiency of the CSF approach, this cut and paste approach also was conducted using these sampled 6,613

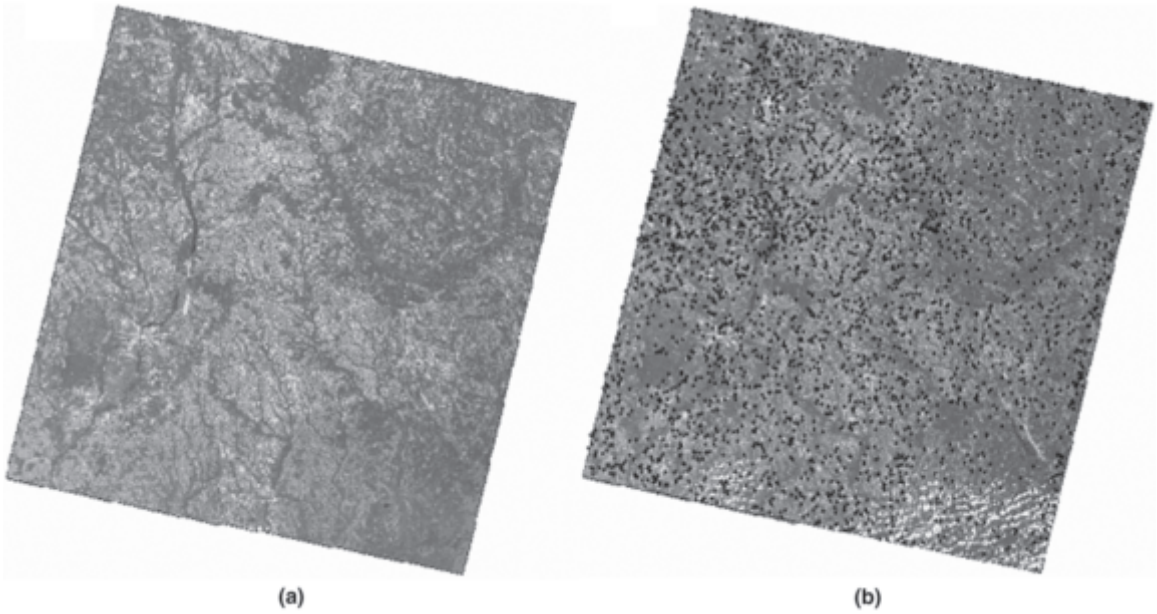

Figure 2. Landsat TM images of Path 18/Row 38 with latitude/longitude centroids of 31.75/ −83.58. Bands 4, 3, and 2 were portrayed as R-G-B, respectively:(a) the base image after removing clouds and cloud shadows, and (b) randomly sampled pixels (black dots) used to check accuracy. A color version of this figure is available at the ASPRS website: **www.asprs.org**.

pixels. The CSF technique is compared with the so-called "cut and paste" approach, because both of them are simple. Additionally, both approaches need a common prerequisite of an auxiliary image, and there are not apparent overlaps of CCS areas in the base image and auxiliary image.

Some statistics are applied to check the errors. Errors are checked using bias (BS) and mean absolute error (MAE). Other criteria including the standard deviation of the errors (SD), relative bias (RBS), relative MAE (RMAE), and ratio of errors (ROE) also are used to compare values between the forecasted DN (i.e., the most similar pixel *B*) obtained using CSF and the DN (i.e., *A*) in the base image. Bias error is used to measure either under-forecast or over-forecast of a parameter, and it is defined by the equation:

$$BS(X) = \frac{1}{N}\sum_{n=1}^{N}(X_f - X_o) \tag{2}$$

where N is the total number of comparisons, X is the band of Landsat imagery, X_f is the forecast value, and X_o is the observed value. A positive BE indicates a tendency to over-forecast while a negative BE implies under-forecasts.

Mean-absolute error is the average of the absolute value of the difference between forecasts and observed pixel values as defined by Equation 3. Values of MAE close or equal to 0 indicate perfect or almost perfect forecasts.

$$MAE = \frac{1}{N}\sum_{n=1}^{N}|X_f - X_o| \tag{3}$$

The SD is defined using Equation 4. The larger the SD, the broader the dispersion of error is from its mean:

$$SD = \left[\frac{1}{N-1}\sum_{n=1}^{N}(E_n - \overline{E})^2\right]^{1/2} \tag{4}$$

where N is the sample size (i.e., the numbers of sampled pixels), E_n is the error values, and $\overline{E}$ is the mean of the errors.

The relative errors and ratio of errors are calculated using the following equations:

$$RBS = \frac{BS(X)}{\overline{X}} * 100 \tag{5}$$

$$RMAE = \frac{MAE(X)}{\overline{X}} * 100 \tag{6}$$

$$ROE = \frac{Error\ from\ cut\ \&\ paste}{Error\ from\ CSF}. \tag{7}$$

The errors of forecasts (bias and MAE), standard deviation of errors, the relative errors (RBS, RMAE, and ROE), and the mean and stand deviation of the seven bands were listed in Table 1. Using CSF approach, we get very small BS (from −0.05 to 1.63) and MAE (from 1.5 to 9.56). Using the cut and paste approach, we obtained much larger BS (from 3.63 to 52.6) and MAE (from 12.07 to 53.28). The relative bias using CSF approach is from 0.06 to 1.11 percent, while it is from 12.61 to 56.07 percent using cut and paste approach. The relative MAE is from 1.06 to 22.09 percent using CSF approach, while it is from 25.84 to 56.8 percent using cut and paste approach. The ratio of errors indicate that bias from cut and paste approach is at least 11 times as large as that from CSF approach, and the MAE from cut and paste approach is at least 2 times as large as that from CSF approach. This error analyses indicate that the CSF approach results in small errors, and it is simple and powerful for removing CCS pixels in Landsat imagery.

Example Two: Test CSF using QuickBird and MODIS Images

We then used QuickBird and MODIS images to check the performance of CSF for CCS pixel removal. Two-scene

TABLE 1. THE EFFICIENCY OF CLOUDS AND CLOUD SHADOWS REMOVAL USING CSF

		Band 1	Band 2	Band 3	Band 4	Band 5	Band 6	Band 7
Sampled pixels		(70.63)[a]	30.83	28.79	93.81	84.63	140.99	31.39
		(17.61)[b]	11.91	16.69	27.33	35.13	6.77	20.47
		0.15	−0.05	0.32	0.79	1.63	−0.09	0.20
	CSF	(10.91)[b]	6.19	9.19	8.59	12.50	1.82	7.31
		(0.21)[c1]	0.16	1.11	0.84	1.93	0.06	0.64
BS		14.53	7.29	3.63	52.60	32.27	36.41	8.29
	Cut and paste	(30.52)[b]	16.69	22.90	27.90	33.73	17.75	22.30
		(20.57)[c1]	23.65	12.61	56.07	38.13	25.82	26.41
	ROE	96.87	145.80	11.34	66.58	19.80	404.56	41.45
		7.34	4.50	6.36	6.45	9.56	1.50	5.76
	CSF	(8.07)[b]	4.25	6.64	5.72	8.19	1.04	4.50
		(10.39)[c2]	14.60	22.09	6.88	11.30	1.06	18.35
MAE		24.91	12.07	12.98	53.28	37.70	36.43	15.80
	Cut and paste	(22.85)[b]	13.34	18.35	26.58	27.53	17.71	17.79
		(35.27)[c2]	39.15	45.09	56.80	44.55	25.84	50.33
	ROE	3.39	2.68	2.04	8.26	3.94	24.29	2.74

Note: BS is bias, MAE is mean absolute error, ROE is ratio of the error of cut and past to the error of CSF; and CSF is closest spectral fit.
a: mean;
b: standard deviation of the mean;
c1: relative bias (RBS);
c2: relative MAE (RMAE).

QuickBird images (DigitalGlobe, 2004 and 2005) with four bands and 2.79 m pixel size and two-scene MODIS images (NASA, 2004 and 2005) with seven bands and 500 m pixel size were downloaded from the Global Land Cover Facility at the University of Maryland and applied to test the performance of CSF analysis.

We designed the cloudy parts in one scene of QuickBird and MODIS images since all the images are cloud-free images. Those images with pseudo clouds were used as the base images (Figure 3 and 4). The rest of the scene is used as an auxiliary image. We need not do any processing of surface reflectance calculation, since the data are already in the standard level. Identification of CCS pixels is not necessary, because we fabricated the cloud parts in the images and we recorded the locations of the cloud parts. The CSF steps 1, 4, 5, 6 were repeated to process the base image and auxiliary image. Visual comparisons of the assumed cloudy pixels and the predicted pixels of the QuickBird images indicated not much difference, and the fused based image maintained the basic spatial and spectral structure in its original image (Figure 3). Likewise, the CSF for replacing the CCS pixels in MODIS images was also good in visualization (Figure 4).

The relative bias error and the relative absolute error at the per pixel level are summarized in Table 2 and Table 3. We obtained small bias errors and mean absolute errors for QuickBird bands 1, 2, and 3, while the bias error and mean absolute error for band 4 are relatively large (Table 2). The bias errors for MODIS bands 1, 3, 4, 5, 6 are small, but relative mean absolute errors for bands 1, 2, 5, 7 are larger than 30 percent of the band mean values (Table 3). The CSF only performed well for MODIS bands 3, 4, 6, although the relative bias errors are small for the rest of the bands. However, the CSF analysis for the CCS pixels covering only the land areas (i.e., the 25 cloudy regions indicated in light grey circles in Figure 4c) resulted in significant decreases in bias error and mean absolute error for bands 1, 2, 4, 5, and 7, though without significant changes of errors for band 3 and 6 (Table 3). We obtained much larger mean absolute errors in all the MODIS bands using this CSF technique when the rest of the 29 cloudy regions covering ocean areas and coastal lines were analyzed when the bias errors were relatively small in bands 3 and 6 (Table 3 and Figure 4).

Discussion

Computational efficiency is important when the analysis of closest spectral fit is processed. For example, when one scene Landsat TM image is used as auxiliary image for selecting the most similar pixels for a given set of pixels whose location-based one-to-one correspondence are CCS pixels in base image, one temporary file could be as large as 200 GB, and the CSF process was not completed within one week using a computer of Dell DIMENSION 8300, Pentium® 4 CPU 3.00GHZ, and 2.00GB of RAM. Then, a random sample was selected from those cloud-free pixels for the CSF analysis. We compared the sample size of 5,000, 10,000, 20,000, 50,000, and 100,000. The size of 20,000 was used as an optimum sample, since we did not obtain significant differences in closest spectral fit when the sample size was increased to 50,000 and 100,000. If several advanced computers and parallel computation are available, using the whole scene image could improve the closest spectral fit.

The relationship of closest spectral fit in a given pair of base image and auxiliary image should be the same or very similar. The two images covering the same area were obtained using the same remote sensor and had been processed using the same procedures. Both the base image and auxiliary image are collected by the same satellite at the same position but at different times. The original images can really represent the spectral characteristics of the objects on the Earth except the CCS pixels. Therefore, in the auxiliary image, the closest digital numbers (DN) of two pixels a and b indicate the most similar objects on the ground at location i and j; in the base image, the two pixels A and B having the same location i and j as the pixels a and b should still have the closest DN, because the two most similar objects occupying the same location i and j on the ground are assumed to be stable. Once the most similarity relationship of pixel a and b is determined using auxiliary image, we can apply this relationship in base image. Then, CCS pixels are

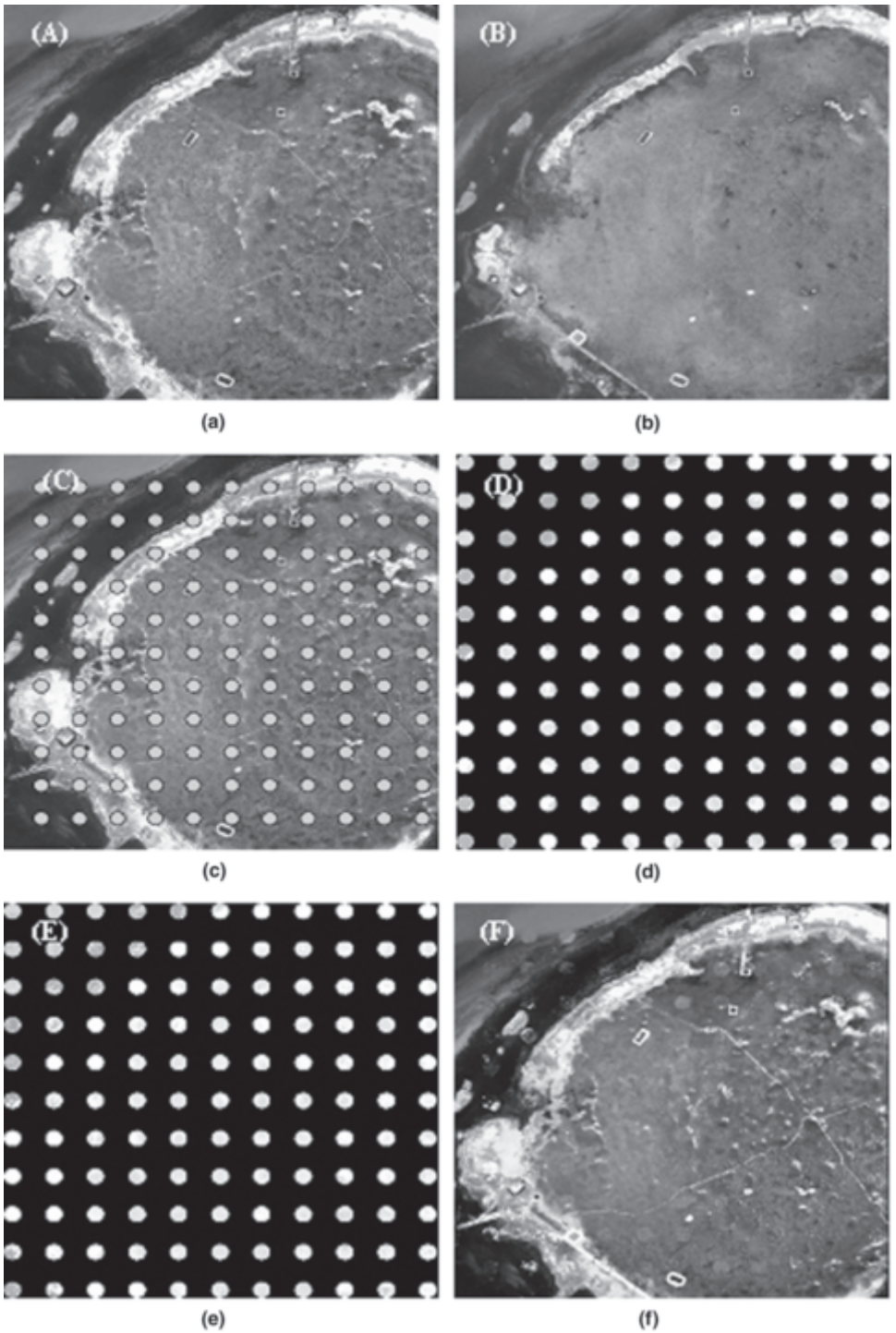

Figure 3. Clouds and cloud shadows removal using QuickBird images (latitude/longitude centroids of 19.68/85.30) with 2.79 m pixel size: (a) the base image obtained on 11 December 2004, (b) the auxiliary image obtained on 31 January 2005, (c) designed 122 cloudy regions using the base image, (d) pixel areas assumed being covered by clouds in the image, (e) predicted pixels for the assumed cloudy areas using the closest spectral fit based on the auxiliary image, and (f) the fused base image using predicted pixels by CSF analysis. A color version of this figure is available at the ASPRS website: **www.asprs.org** .

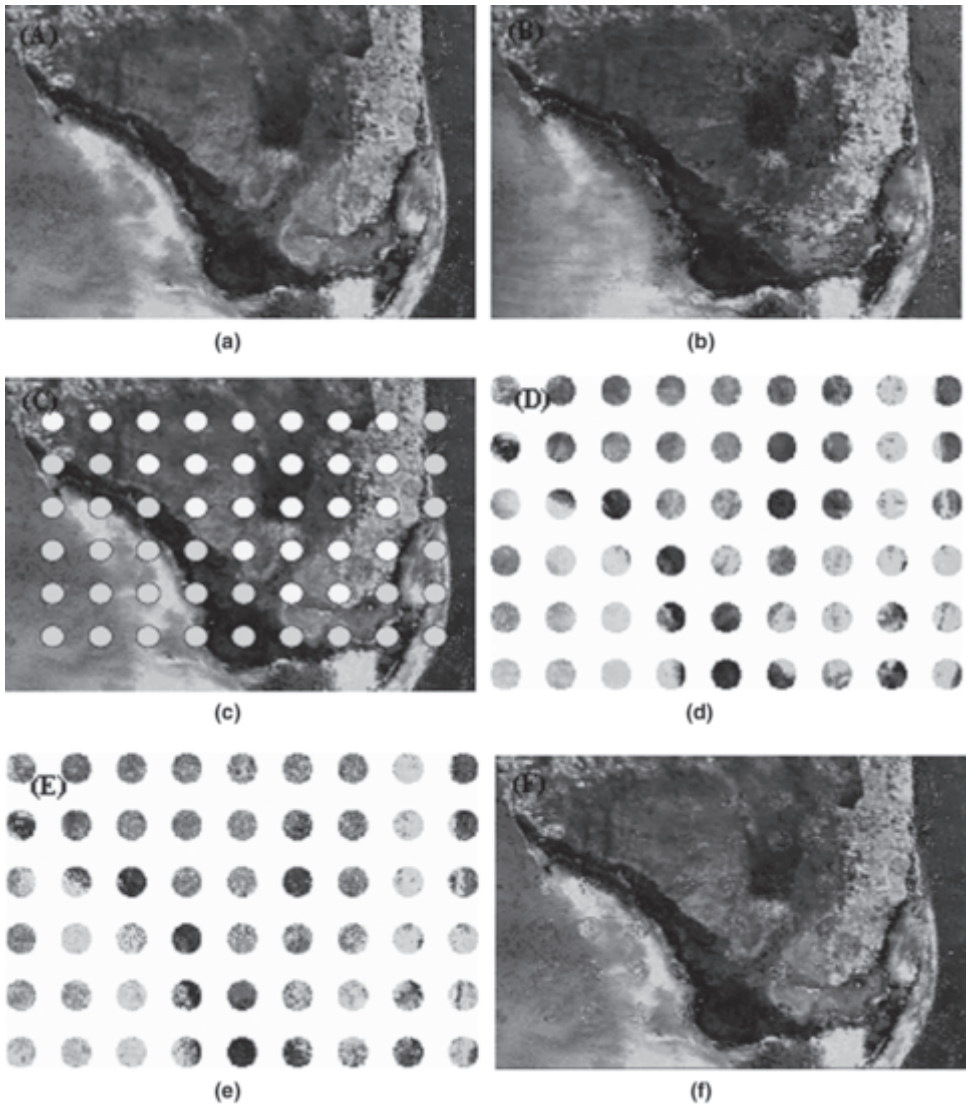

Figure 4. Clouds and cloud shadows removal using MODIS images (latitude/longitude centroids of 25.77/ −80.98) with 500 m pixel size: (a) the base image obtained on 18 March 2005, (b) the auxiliary image obtained on 12 March 2004, (c) designed 54 cloudy regions (i.e., circle regions) including 25 cloudy regions indicated in light grey circles covering the land areas of south Florida and the rest 29 cloudy regions covering ocean and coastal lines, (d) pixel areas assumed covered by clouds in the base image, (e) predicted pixels for the assumed cloudy areas using the closest spectral fit based on the auxiliary image, and (f) the fused base image using predicted pixels by CSF analysis. A color version of this figure is available at the ASPRS website: **www.asprs.org** .

TABLE 2. ERROR DIAGNOSTICS OF CLOSEST SPECTRAL FIT USING QUICK BIRD IMAGES

	Band1	Band2	Band3	Band4
Mean	195	261	148	121
Standard deviation	14	28	26	60
RBS	5.33	7.62	13.24	25.61
RMAE	5.69	8.19	13.98	26.94

Note: RBS, relative bias error; RMAE, relative mean absolute error.

replaced by the most similar pixels in this base image, and the spectral integrity of the base image can be maintained.

However, the objects on the Earth are not always stable or some objects change their locations frequently. For example, about half of the areas in the MODIS images are sea surface water around southern Florida, USA. Components of the surface water are significantly affected by waves, currents, tides, and temperature. In this case, the spectral-based closest fit determined by the auxiliary image may not work well in the base image, because water movement can change its components that significantly change the spectral

TABLE 3. CLOSEST SPECTRAL FIT ANALYSIS USING MODIS IMAGES

Mean	5585	12394	287	564	9358	1084	766
Standard deviation	17602	24061	167	1888	20801	894	3280
RBS	7.75	20.92	3.24	12.05	10.32	0.83	18.92
RMAE	45.21	30.32	21.25	23.93	56.63	17.52	36.42
RBS*	0.19	0.24	4.12	3.17	0.57	3.01	3.66
RMAE*	1.31	1.82	24.39	18.39	3.96	20.69	26.07
RBS**	9.73	9.44	3.33	6.57	5.24	1.01	64.59
RMAE**	80.17	77.95	29.90	49.26	113.86	16.33	87.89

Note: RBS, relative bias error; RMAE, relative mean absolute error.
*: error diagnostics for the 22 pseudo cloudy regions covering the land areas in MODIS image.
**: error diagnostics for the 32 pseudo cloudy regions covering the sea areas in MODIS image.

characteristics of surface water (e.g., the object of the sea surface is changing every second). The similarity relations between two given locations (e.g., two pixels) in the base image can be significantly different from that of the same two locations in the auxiliary image, because water components are significantly changed as time passes. This can be the main reason that the CSF cannot perform well when the MODIS image covering a large sea area was analyzed. This coincides with the significant differences in the errors of cloud removal between land areas and ocean areas in the MODIS images. However, the example using QuickBird images locating also in a costal area and covering parts of the Chilka Lake in India indicates good fused images using the predicted pixels. All in all, whether CSF performs well for given ocean images mainly depends on the significant changes of water components because of the currents, waves, and tides.

Conclusions

A closest spectral fit technique has been developed and conducted in order to remove CCS and to compose cloud-free images. The examples and diagnostic checks indicate that the CSF technique is an efficient approach. This CSF technique is not complex and is easy to understand, and using it generally includes six steps. The six steps of CSF analysis are needed to be repeated when an additional auxiliary image is added to help remove possible overlaps of clouds or cloud shadows in a given pair of base and auxiliary images. The additional auxiliary images can be called 2nd, 3rd, or 4th auxiliary images and so on until there is no overlap of clouds and cloud shadows between the base image and the auxiliary images.

A knowledge-based CCS pixel identification is used to identify and segment clouds and cloud shadows. The threshold of 95 for Landsat TM band 1 was used for detecting clouds. The threshold of Landsat TM band 4 (i.e., 55) and the ratio (i.e., 1.3) of Landsat TM band 4 to band 3 were used to distinguish cloud shadows in satellite imagery. This ratio improved the discrimination between cloud shadows and water areas. The three criteria are flexible and adjustable from image to image.

The error diagnostics using Landsat TM, QuickBird, and MODIS images indicates that the technique of closest spectral fit is a relatively accurate approach to remove clouds and cloud shadows from images. Compared with other cloud removal methods discussed above, one advantage of closest spectral fit is that its efficiency (i.e., the accuracy of removing clouds and cloud shadows) can be diagnostically checked when it is applied. A statistical check of errors in predicting band values indicates whether this band could be used for further applications. Another advantage is that the CSF technique does not depend on the areas, the thickness, and the density of clouds and cloud shadows in the images.

Acknowledgments

Thanks go to Dr. E. Lynn Usery for his review and advice on an earlier version of this manuscript. The authors also thank Dr. James W. Merchant and three reviewers for their helpful comments.

References

Caselles, V., 1989. An alternative simple approach to estimate atmospheric correction in multitemporal studies, *International Journal of Remote Sensing*, 10(6):1127–1134.

Chanda, B., and D.D. Majumder, 1991. An iterative algorithm for removing the effects of thin cloud cover form Landsat imagery, *Mathematical Geology*, 23(6):853–860.

Cihlar, J., and J. Howarth, 1994. Detection and removal of cloud contamination from AVHRR images, *IEEE Transactions on Geoscience and Remote Sensing*, 32(3):583–589.

DigitalGlobe, 2005, QuickBird scene 000000185964_01_p006, Level Stand 2A, DigitalGlobe, Longmont, Colorado, 01 January.

DigitalGlobe, 2004, QuickBird scene 000000185964_01_p003, Level Stand 2A, DigitalGlobe, Longmont, Colorado, 01 January.

ITT Company, ENVI Add-Ons FLAASH, URL: *http://www.ittvis.com/envi/flaash.asp* (last date accessed: 31 January 2009).

Liu, Z.K., and B.R. Hunt, 1984. A new approach to removing cloud cover from satellite imagery, *Computer Vision, Graphics, and Image Processing*, 25:252–25.

Mitchell, O.R., E.J. Delp, III, and P.L.Chen, 1977. Filtering to remove cloud cover in satellite Imagery, *IEEE Transactions on Geoscience Electronics*, GE-15(3):137–141.

NASA, 2005, MODIS 16-day Composite MOD44C, Collection 4, The Global Land Cover Facility, University of Maryland, College Park, Maryland.

NASA, 2004, MODIS 16-day Composite MOD44C, Collection 4, The Global Land Cover Facility, University of Maryland, College Park, Maryland.

Simonett, D.S., 1983. *Theory, Instruments, and Techniques - Volume 1 of the Manual of Remote Sensing*, Falls Church, Virginia: American Society of Photogrammetry, 170 p.

Simpson, J.J., and J.R. Stitt, 1998. A procedure for the detection and removal of cloud shadow form AVHRR data over land, *IEEE Transactions on Geoscience and Remote Sensing*, 36(3):880–897.

Song, M., and D.L. Civco, 2002. A knowledge-based approach for reducing cloud and shadow, *Proceedings of the 2002 ASPRS-ACSM Annual Conference and FIG XXII Congress*, Washington, D.C., 22–26 April.

U.S. Geological Survey. Thematic Mapper Product Description, URL: *http://edc.usgs.gov/products/satellite/tm.html* (last date accessed: 31 January 2009).